Fabrication and Characterization of Gold–Polymer Nanocomposite Plasmonic Nanoarrays in a Porous Alumina Template

Shobha Shukla,[†,§] Kyoung-Tae Kim,[†] A. Baev,[§] Y. K. Yoon,[†] N. M. Litchinitser,[†] and P. N. Prasad[†,‡,§,*]

[†]Department of Electrical Engineering, [‡]Department of Chemistry, and [§]Institute of Lasers, Photonics and Biophotonics, University at Buffalo, The State University of New York, Buffalo, New York 14260

ABSTRACT A facile, cost-effective, and manufacturable method to produce gold–polymer nanocomposite plasmonic nanorod arrays in high-aspect-ratio nanoporous alumina templates is reported, where the formation of gold nanoparticles and the polymerization of a photosensitive polymer by ultraviolet light are simultaneously performed. Transverse mode coupling within a two-dimensional array of the nanocomposite rods results in a progression of resonant modes in the visible and infrared spectral regions when illuminated at normal incidence, a phenomenon previously observed in nanoarrays of solid gold rods in an alumina template. Finite element full-wave analysis in a three-dimensional computational domain confirms our hypothesis that nanoparticles, arranged in a columnar structure, will show a response similar to that of solid gold rods. These studies demonstrate a new simple method of plasmonic nanoarray fabrication, apparently obviating the need for a cumbersome electrochemical process to grow nanoarrays.

KEYWORDS: nanocomposite · nanoarray · nanoparticles · plasmons · AAO · optical properties

Recently, there has been a great deal of interest in plasmonic properties of coupled gold nanostructures as they possess unique electronic and magnetic properties and have potential for a wide variety of applications such as biosensing, diagnostics, band-pass filtering, imaging beyond diffraction limit, *etc.*[1–5] Plasmonic nanostructures are very attractive due to ability to tune their plasmonic response by changing their geometry.[6] Due to the anisotropy and susceptibility to the local environment, investigations have been recently extended to the interfacial phenomena, giving rise to new variety of applications such as fluorescence enhancements, surface-enhanced Raman scattering (SERS), *etc.*[7,8] Gold–dielectric interfaces support coherent excitation of electron density oscillations in the metal and thus enhancing the local field strength.[1,6,9–11]

In producing plasmonic nanostructures, one has to have a precise control of size, shape, and interparticle distance in order to attain a specific plasmon mode because it arises from the hybridization of primitive plasmon modes.[12,13] There have been attempts to periodically arrange metal nanostructures in order to achieve pronounced localized surface plasmon resonances and produce an intense electromagnetic field extended well beyond their physical dimensions.[1,12,14–17] By controlling the dielectric environment around periodically arranged anisotropic metal nanostructures, one can obtain even more dramatic plasmonic properties and tunability.[3,18] Top-down approaches such as e-beam lithography or focused ion beam lithography are excellent in producing periodic nanostructures, but the throughput is limited. A bottom-up approach such as self-assembly can produce closely packed two-dimensional (2D) and three-dimensional (3D) structures of nanoparticles, but periodically arranging anisotropic particles is still challenging.[19,20] There are reports on the fabrication of ordered one-dimensional (1D) plasmonic structures, but commercially viable fabrication of ordered structures is yet to come.[16,21] In the meantime, template-mediated fabrication is one of the effective methods to produce ordered arrays. Anodized aluminum oxide (AAO) templates have been used as a direct route to produce ordered structures of various materials with fine size controllability on large size scale.[10] By controlling the allowed oxidation time, applied voltage, and different types of acids, the pore geometry of an AAO template can be varied. An electrochemical deposition method to fill the AAO template is normally used to produce metallic nanorod arrays in the template.[20,22]

*Address correspondence to pnprasad@buffalo.edu.

Received for review December 1, 2009 and accepted March 04, 2010.

Published online April 12, 2010.
10.1021/nn9018398

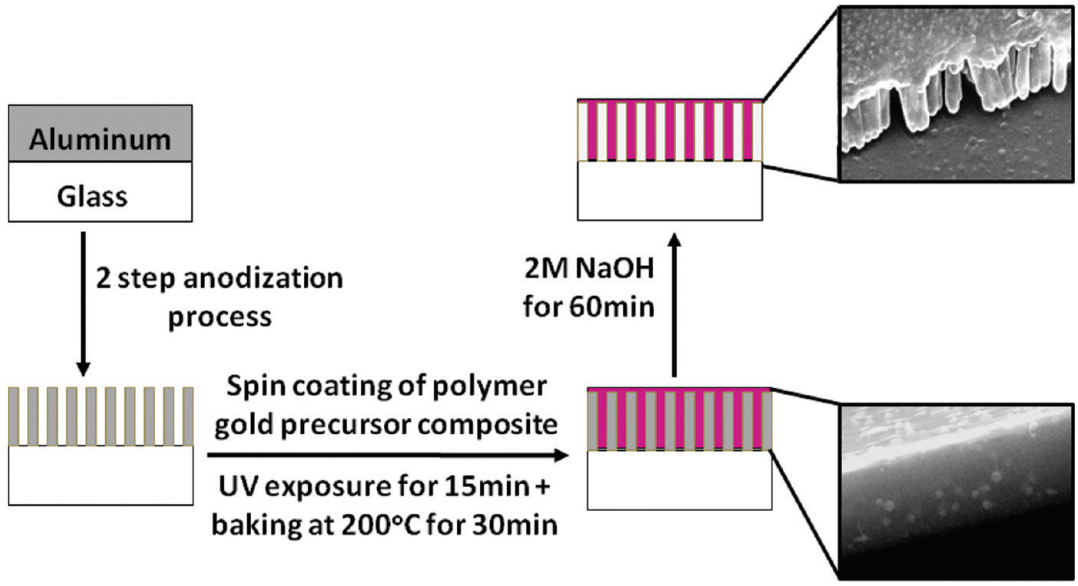

Figure 1. Schematic of the fabrication process.

However, during the electrodeposition process, variable or poor ohmic contact is a challenge in the homogeneous growth of a nanostructure in the template.[20]

Keeping all of the above-mentioned factors in mind, we developed a facile, cost-effective, and manufacturable method for the template-directed synthesis of vertically arranged gold−polymer composite plasmonic nanostructures by *in situ* photoreduction of a gold precursor and simultaneous photopolymerization of the polymer during ultraviolet (UV) light exposure. Template pore dimension is varied to tune the aspect ratio of plasmonic structures. Plasmonic responses of the as-produced plasmonic nanoarray were studied and found to be in good agreement with those of theoretical calculation. We have successfully shown that the optical response of the gold nanoparticle−polymer composite nanoarray in an AAO template is similar to the response of a solid gold nanorod array in an AAO template.

RESULTS AND CHARACTERIZATION

Figure 1 shows the schematic of the process for plasmonic array fabrication in an AAO template. Figure 2a−c shows the different hole sizes in an AAO template varying from 20 to 70 nm. Hole sizes were increased by increasing the bias voltage and the pore widening time in 5 weight % phosphoric acid.[19] The AAO template filled with gold-nanoparticle-doped SU8 is shown in Figure 2d,e. The inset of Figure 2d is the secondary electron emission image of the same sample, whereas Figure 2e shows the backscattered SEM of the distant view of the gold-nanoparticle-doped SU8 in an AAO template. The inset of Figure 2e shows a side view of the fabricated bare AAO template. The size of the gold nanoparticles in the array was found to be in the range of 20−40 nm. When the sample was heated above the glass transition temperature (65 °C),[23] SU8 starts to flow; due to the capillary action, composite material goes inside the holes of the AAO template filling it completely. From the backscattered electron emission images (Figure 2d,e), we confirmed that the spherical structures were gold nanoparticles, with a thin layer of composite material on the top of the AAO template. This thin layer serves as a support base for the free-standing composite nanorod array. Some big nanoparticles (~100 nm) were also found in the top supporting layer.[24]

The optical characterization of the plasmonic nanoarray is shown in Figure 3. For the reference, we made a thin film of the gold precursor−SU8 composites and recorded the reflectance spectra before UV exposure and after UV exposure; the appearance of a dip at 510 nm, which is a characteristic of the gold nanoparticle plasmonic resonance, confirms *in situ* gold reduction (see the Supporting Information Figure S1). A bare AAO template shows few peaks in reflectance depending on the size of the hole. We tentatively attribute these spectral features to the photonic band gaps of our quasi-periodic two-dimensional photonic crystal-like structures.[25] The broadening of the peaks can be related to poor long-range periodicity in this case. As the aspect ratio (AR) was decreased from 20 to 4 (with hole size variation = 20 ± 5, 40 ± 5, 60 ± 5, 70 ± 5, 80 ± 5, and 100 ± 5 nm with fixed height of 400 nm), the peaks shift from the visible region to the NIR region, with comparatively richer spectral features, as shown in the top panel of Figure 3a,b. Optical response of the composite nanoarrays highly depends on the hole sizes of the template. Because it is very difficult to achieve the same hole size after etching, optical response varies a little from one batch to another batch but the trend remains the same. Numerical simulations (see

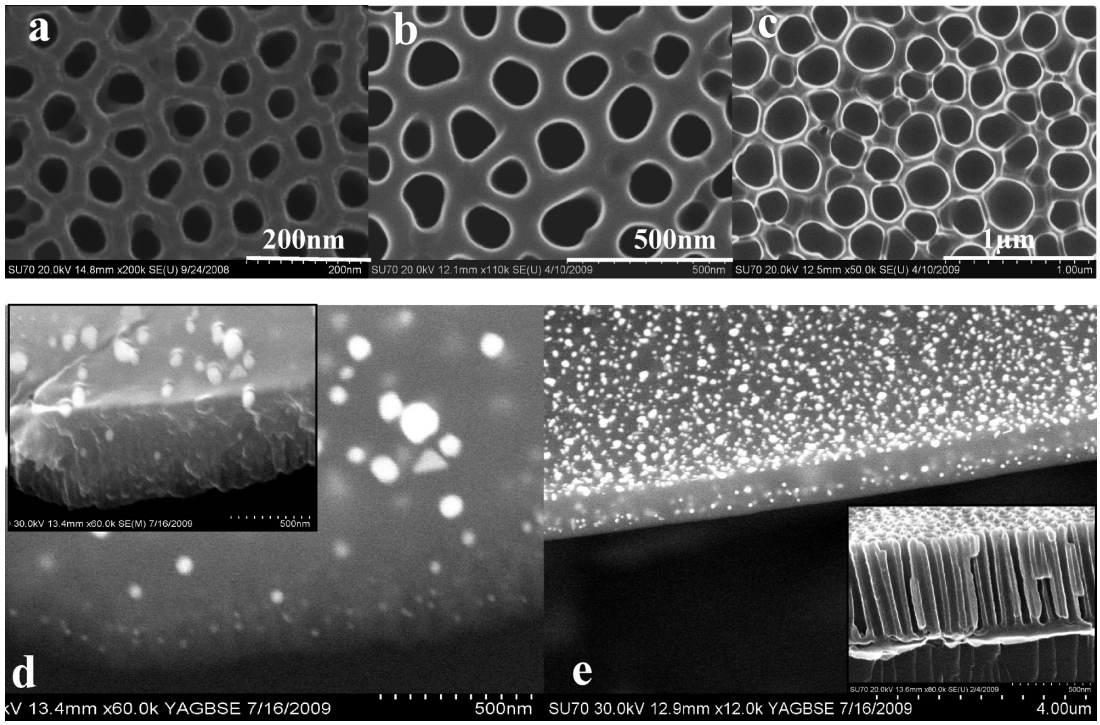

Figure 2. (a−c) SEM images of the AAO template with three different hole sizes. (d) Backscattered emission SEM image of an AAO template with a plasmonic array (inset: secondary emission SEM image of the same). (e) Distant view of backscattered emission SEM image of a plasmonic array in an AAO template (inset: bare AAO template).

the Supporting Information Figure S5) showed that multiple reflections from the dielectric interfaces result in a rich pattern of interference fringes, something we did not observe in our measurements. The roughness of the surface could be the reason for the observed broadening and wash-off of the fringes.

Vertically aligned composite nanoarrays show the optical response (Figure 3, lower panels), similar to that of solid gold rod nanoarrays in an AAO template, as shown by Lyvers *et al.*[26] Thus, our process obviates the need for cumbersome processing to get plasmonic nanoarrays. The composite plasmonic nanoarrays produced from a smaller hole size AAO template (high aspect ratio of the rods) show less resonant peaks as compared to the ones made out of a template with bigger hole sizes (lower panel of Figure 3a,b). This observation is different from that of Lyvers *et al.*,[26] who showed that gold nanorods, electrochemically grown in an AAO template, will exhibit more resonances in reflection with an increase in the aspect ratio (increasing height of the plasmonic array keeping hole radius constant). Because we varied the aspect ratio by increasing the hole radius (keeping height constant), we got more resonances at a low aspect ratio. To further bolster these inferences, we performed numerical simulations of reflectance.

Reflectance spectra of fabricated arrays were simulated using finite element analysis (FEA) implemented

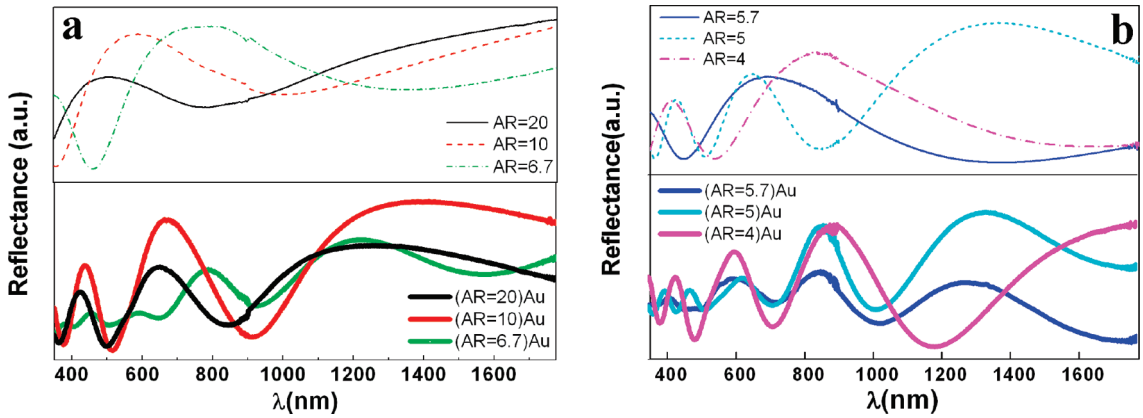

Figure 3. Reflectance spectra of the plasmonic nanoarrays in the AAO template. Top part of a and b: aspect ratio (AR) of a bare AAO template was decreased progressively from 20 to 4. Bottom part of a and b: (AR=20)Au to (AR=4)Au are the reflectance spectra with gold nanoparticle arrays in an AAO template with the corresponding aspect ratios (aspect ratio = height/diameter).

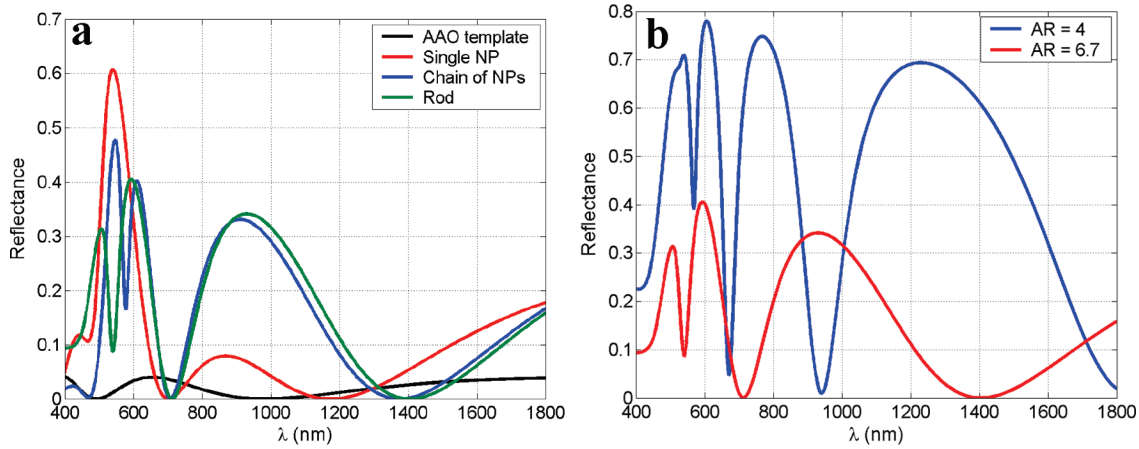

Figure 4. (a) Simulated reflectance spectra of the AAO template and different plasmonic arrays. The AAO hole radius is 50 nm in all cases. The gold NP radius is 30 nm in all cases. The rod aspect ratio is 6.7. (b) Simulated reflectance spectra of plasmonic arrays with different aspect ratios of the rods.

in a COMSOL software package. The double periodic boundary conditions ensured an infinite 2D array with triangular lattice and the unit cell size of $a(3/2 \times a/2)^{1/2}$, where $a = 130$ nm is the lattice constant (center-to center distance between the holes). The height of the array was set to 400 nm. Far-field reflectance/transmittance was estimated at a distance of 2 μm from the confining surfaces of the array. The incident electric field was *x*-polarized. The dielectric properties of gold were described by the Drude function adjusted for the visible−near-infrared region.[27,28] The results of simulations are presented in Figure 4. For the sake of clarity, we performed the simulations without the glass substrate. In this case, the number of interference fringes is drastically reduced (see Figure 4a, black curve). It is worthwhile to note that in the simulations the incident field is propagating perpendicular to the air−AAO interface (normal incidence). This allows elimination of any photonic crystal effects and focuses our attention on plasmonic coupling effects because the light does not couple to the guided modes of the crystal. In the experiment, however, there is a small angle of 2.5° between the normal to the interface and the wavevector because of the setup configuration. This can contribute to the difference between reflectance spectrum obtained for empty AAO templates (Figures 3 and 4). Lyvers *et al.*[26] reported that increasing the aspect ratio at a given hole size results in multiplying the number of resonances per wavelength interval. This trend is reversed in our case, where the aspect ratio is increased at the expense of a smaller hole size at the given height of an AAO template (we always keep the lattice constant fixed in our simulations, thereby the volume fraction of gold changes with a change in the hole size). In this case, the smaller number of resonances in reflection can be attributed to weaker coupling between the transverse modes of individual nanorods. This observation is supported by our simulations. In Figure 4b, for the sample with AR = 4, the resonances are red-shifted with respect to AR = 6.7, and additional resonances rise in the visible part of the spectrum. This shift/additional resonances can be attributed to a strong retardation effect, making better transverse mode coupling between the propagating modes. AR = 4 well represents the graph corresponding to (AR=4)Au in Figure 3b, and AR = 6.7 corresponds to graph (AR=6.7)Au in Figure 3a.

Comparison of simulated curves (Figure 4a) with experimental reflectance curves shown in Figure 3 supported our conclusion about the plasmonic rod-like nature of the composite inside the AAO pores. Plasmonic nanoparticles arranged into chain/columnar structures inside AAO pores respond to the incident light in a manner similar to that of solid gold rods due to evanescent field coupling between the gold nanoparticles, which makes the electron density within all of the nanoparticles oscillate in phase.[29] At the same time, the response of a single gold sphere, equivalent to the response of non-interacting particles inside AAO channels, differs drastically, showing only one strong resonance in the visible (Figure 4a). The prominent blue shift (40 nm) of the first resonant peak in the case of solid rods compared to the chain of spheres (AR = 4, AR = 6.7) or a single sphere can probably be attributed to the spectral shift between the primitive localized transverse resonances of a sphere and a cylinder with AR = 1. As we mentioned earlier, the multiple resonances in reflectance are attributed to strongly coupled transverse modes between closely spaced composite nanorods, an effect analogous to photonic mode waveguided in an anisotropic slab.[26] Each resonance corresponds to a longitudinal standing wave, excited and confined between nanorods. Measurements with a bare substrate, as a control sample, have also been performed to confirm that optical responses from the nanoarray arise essentially from resonant backscattering.

The AAO template-released plasmonic nanoarrays are shown in Figure 5a,b. The inset shows a close up view of the free-standing plasmonic array. It is very

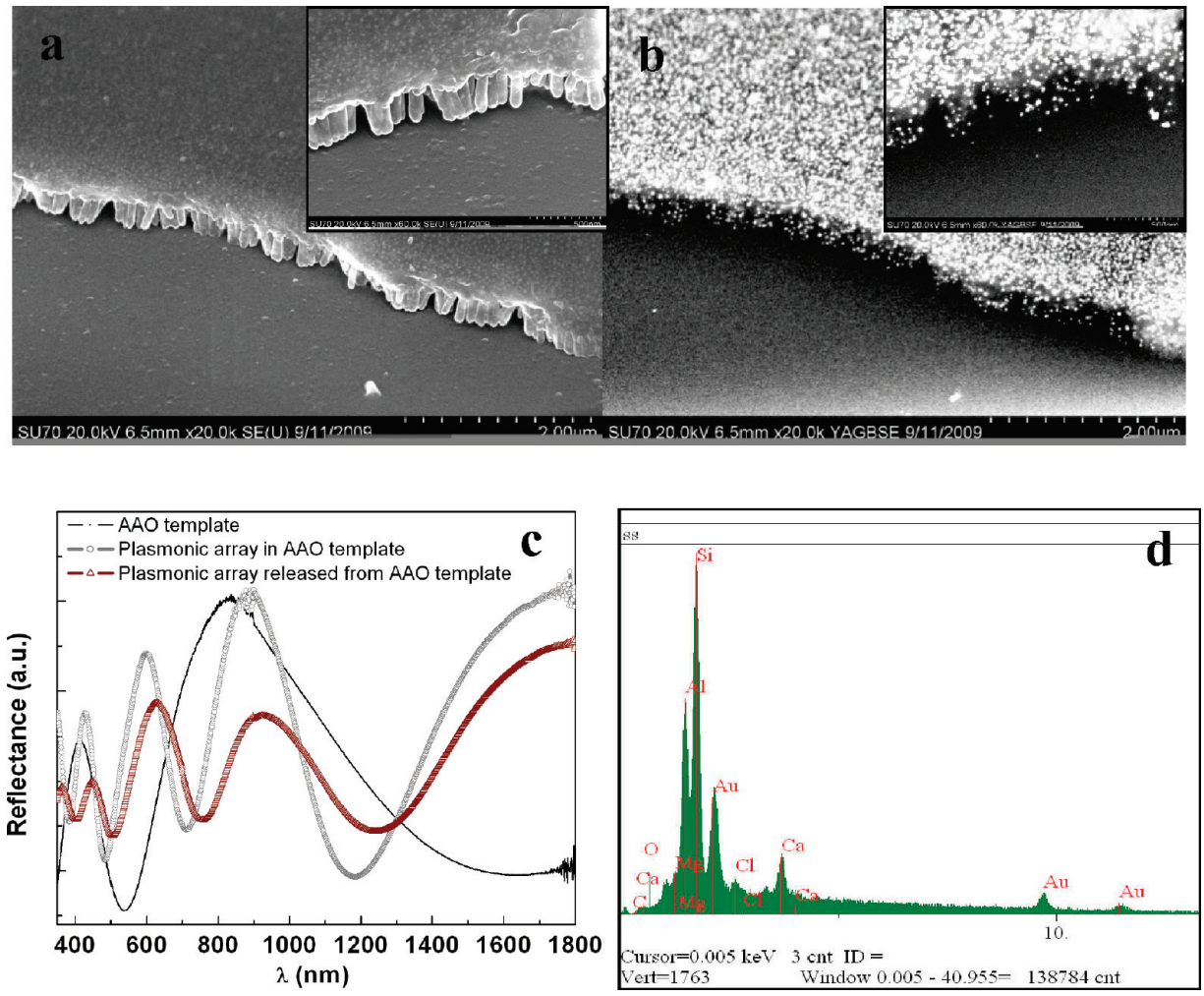

Figure 5. AAO template-dissolved free-standing plasmonic nanoarrays. (a) Secondary emission SEM image of the array. (b) Backscattered SEM image of the same (inset: close up view of the same sample in secondary emission and backscattered emission SEM images). (c) Optical response of the plasmonic array released from the alumina template. (d) EDS spectra of the plasmonic array. Scale bar in a and b = 2 μm; scale bar in inset of a and b = 500 nm.

clear from the images that the template can be removed fully without significantly affecting the plasmonic array. We have recorded the reflectance spectra after dissolving the template to see the effect on optical response (Figure 5c). It is evident from the reflectance spectra that the optical response is practically unaffected by the template removal. A moderate red shift (around 70 nm) of the resonant peaks is the net effect of two competing phenomenon: reduced mean refractive index leads to the blue shift in the spectrum, while local aggregation of template-released rods leads to the red shift.[26,30] It should also be noted that dispersion of longer wavelength resonances is larger than that at the shorter wavelength resonances,[26] which can in principle result in a red shift for longer wavelength peaks and a blue shift or no shift for shorter wavelength ones. In our case, the local aggregation effect is much stronger (as evident from the SEM images), leading to the red shift of the resonances; a small shift was observed at shorter wavelengths and a comparatively large shift for longer wavelengths. EDS has also been performed to cross check the presence of gold nanoparticles. Because the substrate is glass, many other peaks other than gold are in the EDS spectra (Figure 5d).

CONCLUSION

Results presented here illustrate that the plasmonic nanoarrays can be fabricated in alumina templates without cumbersome preprocessing, and this method obviates the need for having a conductive substrate and using the complex chemistry. We have also shown that a columnar arrangement of metal nanoparticles produces the same optical response as that of the pure metal nanorods. Plasmonic nanoarrays exhibit complex response in the visible and the NIR due to the coupling of transverse modes. We hope that this work will open a new door for research and application in various plasmon-based applications such as biosensing, bandpass filtering, subwavelength integrated optical devices, *etc.*

FABRICATION PROCESS

Nonporous AAO templates were obtained by the anodization of thin aluminum (Al) film on a glass substrate. The Al film was formed by electron beam evaporation on the glass substrate, and anodization was performed in a 0.3 M oxalic acid ($H_2C_2O_4$) solution at various voltages between 40 and 100 V to achieve different pore sizes with a two-step anodization technique.[19] By increasing the applied voltage and etching time, hole sizes of the AAO template can be varied from 20 to 120 nm, keeping the lattice constant fixed. Lattice constant can be varied from 100 to 400 nm by changing the etchant (phosphoric acid, sulfuric acid). Small variation in the lattice constant is possible by changing etching temperature, applied voltage, and etchant concentration. A negative photoresist, SU8 (Microchem Inc. SU8-2025), was used as the host matrix for the gold precursor. The gold precursor (Sigma-Aldrich, $HAuCl_4$) was dissolved in cyclopentanone. Ten milligrams of gold precursor was added to 100 mg of SU8 to get 10 weight % of metal nanoparticle for a conducting path in the matrix. A gold precursor−SU8 composite was stirred and ultrasonicated for 15 and 30 min, respectively. The composite was spin coated on an AAO template at 2000 rpm for 40 s. Spin coating speed was carefully adjusted to remove the excess composite material from the template. After spin coating, the sample was irradiated with UV light (i-line, $\lambda = 365$ nm) for 15 min, and sample was baked at 200 °C for 30 min to complete the polymerization/photoreduction process. After cooling, 2 M NaOH was used to dissolve the AAO template to release the free-standing polymer−gold nanoparticle composite. The sample was stored in a desiccator for further characterization.

Composite nanostructures were structurally characterized by scanning electron microscopy (SEM) in the backscattered regime as well as in the secondary electron emission regime and by the EDS (energy-dispersive X-ray system). Optical properties of the sample were studied by measuring spectral reflectance using a UV−vis spectrophotometer in the wavelength range from near-infrared to ultraviolet. The incidence angle was set to 2.5° with respect to the normal to the patterned surface.

Acknowledgment. Support by the Air Force Office of Scientific Research (Grant No. FA95500910258) and the National Science Foundation (CAREER ECCS 0748153) is acknowledged.

Supporting Information Available: Reflectance spectra of SU8−Au precursor unexposed and UV exposed, SEM image of the nanocomposite in an AAO template, AAO template-dissolved free-standing plasmonic nanoarrays, plasmonic array coming out of an AAO template, released plasmonic structures with fully dissolved template, plasmonic nanoarrays fully released from the template, simulated reflectance spectra of a plain alumina slab and of an AAO template on a glass substrate, simulated longitudinal standing waves (harmonics) confined between nanorods in an AAO template. This material is available free of charge *via* the Internet at http://pubs.acs.org.

REFERENCES AND NOTES

1. Prasad, P. N. *Nanophotonics*; John Wiley & Sons: New York, 2004.
2. Jana, N. R.; Gearheart, L.; Murphy, C. J. Seed-Mediated Growth Approach for Shape-Controlled Synthesis of Spheroidal and Rod-like Gold Nanoparticles Using a Surfactant Template. *Adv. Mater.* **2001**, *13*, 1389–1393.
3. Yang, L.; Cai, Q.; Yu, Y. Size-Controllable Fabrication of Noble Metal Nanonets Using a TiO_2 Template. *Inorg. Chem.* **2006**, *45*, 9616–9618.
4. Li, Z.; Hao, F.; Huang, Y.; Fang, Y.; Nordlander, P.; Xu, H. Directional Light Emission from Propagating Surface Plasmons of Silver Nanowires. *Nano Lett.* **2009**, *9*, 4383–4386.
5. Cheng, Y.; C. Samia, A.; Meyers, J. D.; Panagopoulos, I.; Fei, B.; Burda, C. Highly Efficient Drug Delivery with Gold Nanoparticle Vectors for *In Vivo* Photodynamic Therapy of Cancer. *J. Am. Chem. Soc.* **2008**, *130*, 10643–10647.
6. Chen, X. W.; Sandoghdar, V.; Agio, M. Highly Efficient Interfacing of Guided Plasmons and Photons in Nanowires. *Nano Lett.* **2009**, *9*, 3756–3761.
7. Ming, T.; Zhao, L.; Yang, Z.; Chen, H.; Sun, L.; Wang, J.; Yan, C. Strong Polarization Dependence of Plasmon-Enhanced Fluorescence on Single Gold Nanorods. *Nano Lett.* **2009**, *9*, 3896–3903.
8. Neretina, S.; Dreaden, E. C.; Qian, W.; El-Sayed, M. A.; Hughes, R. A.; Preston, J. S.; Mascher, P. The Dependence of the Plasmon Field Induced Nonradiative Electronic Relaxation Mechanisms on the Gold Shell Thickness in Vertically Aligned CdTe−Au Core−Shell Nanorods. *Nano Lett.* **2009**, *9*, 3772–3779.
9. Evans, P. R.; Wurtz, G. A.; Atkinson, R.; Hendren, W.; O'Connor, D.; Dickson, W.; Pollard, R. J.; Zayats, A. V. Plasmonic Core/Shell Nanorod Arrays: Subattoliter Controlled Geometry and Tunable Optical Properties. *J. Phys. Chem. C* **2007**, *111*, 12522–12527.
10. Sander, M. S.; Tan, L. S. Nanoparticle Arrays on Surfaces Fabricated Using Anodic Alumina Films as Templates. *Adv. Funct. Mater.* **2003**, *13*, 393–397.
11. Xi, D.; Pei, Q. *In Situ* Preparation of Free-Standing Nanoporous Alumina Template for Polybithiophene Nanotube Arrays with a Concourse Base. *Nanotechnology* **2007**, *18*, 095602–095607.
12. Lassiter, J. B.; Knight, M. W.; Mirin, N. A.; Halas, N. J. Reshaping the Plasmonic Properties of an Individual Nanoparticle. *Nano Lett.* **2009**, *9*, 4326–4332.
13. Le, F.; Brandl, D. W.; Urzhumov, Y. A.; Wang, H.; Kundu, J.; Halas, N. J.; Aizpurua, J.; Nordlander, P. Metallic Nanoparticle Arrays: A Common Substrate for Both Surface-Enhanced Raman Scattering and Surface-Enhanced Infrared Absorption. *ACS Nano* **2008**, *2*, 707–718.
14. Chan, Y.-H.; Chen, J.; Wark, S. E.; Skiles, S. L.; Son, D. H.; Batteas, J. D. Using Patterned Arrays of Metal Nanoparticles to Probe Plasmon Enhanced Luminescence of CdSe Quantum Dots. *ACS Nano* **2009**, *3*, 1735–1744.
15. Losic, D.; Shapter, J. G.; Mitchell, J. G.; Voelcker, N. H. Fabrication of Gold Nanorod Arrays by Templating from Porous Alumina. *Nanotechnology* **2005**, *16*, 2275–2281.
16. Veinot, J. G. C.; Yan, H.; Smith, S. M.; Cui, J.; Huang, Q.; Marks, T. J. Fabrication and Properties of Organic Light-Emitting Nanodiode Arrays. *Nano Lett.* **2002**, *2*, 333–335.
17. Wang, W.; Summers, C. J.; Wang, Z. L. Large Scale Hexagonal-Patterned Growth of Aligned ZnO Nanorods for Nano-optoelectronics and Nanosensor Arrays. *Nano Lett.* **2004**, *4*, 423–426.
18. Oldenburg, S. J.; Averitt, R. D.; Westcott, S. L.; Halas, N. J. Nanoengineering of Optical Resonances. *Chem. Phys. Lett.* **1998**, *288*, 243–247.
19. Masuda, H.; Nishio, K.; Baba, N. Preparation of Microporous Metal Membrane Using Two-Step Replication of Interconnected Structure of Porous Glass. *J. Mater. Sci. Lett.* **1994**, *13*, 338–340.
20. Moon, J. M.; Wei, A. Uniform Gold Nanorod Arrays from Polyethylenimine-Coated Alumina Templates. *J. Phys. Chem. B* **2005**, *109*, 23336–23341.
21. Gopinath, A.; Boriskina, S. V.; Premasiri, W. R.; Ziegler, L.; Reinhard, B. M.; Dal Negro, L. Plasmonic Nanogalaxies: Multiscale Aperiodic Arrays for Surface-Enhanced Raman Sensing. *Nano Lett.* **2009**, *9*, 3922–3929.
22. Cao, Y.; Mallouk, T. E. Morphology of Template-Grown Polyaniline Nanowires and Its Effect on the Electrochemical Capacitance of Nanowire Arrays. *Chem. Mater.* **2008**, *20*, 5260–5265.
23. Charles, C.; Mark, A. Uncrosslinked SU-8 as a Sacrificial Material. *J. Micromech. Microeng.* **2005**, *15*, N1–N5.
24. He, J.; Kunitake, T.; Nakao, A. Facile *In Situ* Synthesis of Noble Metal Nanoparticles in Porous Cellulose Fibers. *Chem. Mater.* **2003**, *15*, 4401–4406.
25. Hase, M.; Egashira, M.; Shinya, N.; Miyazaki, H.; Kojima, K. M.; Uchida, S. I. Optical Transmission Spectra of Two-Dimensional Quasiperiodic Photonic Crystals Based on

Penrose-Tiling and Octagonal-Tiling Systems. *J. Alloys Compd.* **2002**, *342*, 455–459.
26. Lyvers, D. P.; Moon, J. M.; Kildishev, A. V.; Shalaev, V. M.; Wei, A. Gold Nanorod Arrays as Plasmonic Cavity Resonators. *ACS Nano* **2008**, *2*, 2569–2576.
27. Etchegoin, P. G.; Ru, E. C. L.; Meyer, M. An Analytic Model for the Optical Properties of Gold. *J. Chem. Phys.* **2006**, *125*, 164705–164708.
28. Etchegoin, P. G.; Ru, E. C. L.; Meyer, M. An Analytic Model for the Optical Properties of Gold. *J. Chem. Phys.* **2007**, *127*, 189901-1.
29. Rahachou, A. I.; Zozoulenko, I. V. Light Propagation in Nanorod Arrays. *J. Opt. A: Pure Appl. Opt.* **2007**, *9*, 265–270.
30. Palacios-Lidón, E.; Galisteo-López, J. F.; Juárez, B. H.; López, C. Engineered Planar Defects Embedded in Opals. *Adv. Mater.* **2004**, *16*, 341–345.